In silico leaf venation networks: Growth and reorganization driven by mechanical forces

Francis Corson, Mokhtar Adda-Bedia, Arezki Boudaoud

www.elsevier.com/locate/yjtbi

In silico leaf venation networks: Growth and reorganization driven by mechanical forces

Francis Corson, Mokhtar Adda-Bedia, Arezki Boudaoud

PII: S0022-5193(09)00214-8
DOI: doi:10.1016/j.jtbi.2009.05.002
Reference: YJTBI 5552

To appear in: *Journal of Theoretical Biology*

Received date: 29 July 2008
Revised date: 5 May 2009
Accepted date: 5 May 2009

Cite this article as: Francis Corson, Mokhtar Adda-Bedia and Arezki Boudaoud, In silico leaf venation networks: Growth and reorganization driven by mechanical forces, *Journal of Theoretical Biology*, doi:10.1016/j.jtbi.2009.05.002

In silico leaf venation networks: growth and reorganization driven by mechanical forces

Francis Corson, Mokhtar Adda-Bedia and Arezki Boudaoud

Laboratoire de Physique Statistique, UMR 8550 CNRS / ENS / Paris 6 / Paris 7, 24 rue Lhomond, 75231 Paris Cedex 5, France

Abstract

Development commonly involves an interplay between signaling, genetic expression and biophysical forces. However, the relative importance of these mechanisms during the different stages of development is unclear. Leaf venation networks provide a fitting context for the examination of these questions. In mature leaves, venation patterns are extremely diverse, yet their local structure satisfies a universal property: at junctions between veins, angles and diameters are related by a vectorial equation analogous to a force balance. Using a cell proliferation model, we reproduce *in silico* the salient features of venation patterns. Provided that vein cells are given different mechanical properties, tensile forces develop along the veins during growth, causing the network to deform progressively. Our results suggest that the local structure of venation networks results from a reorganization driven by mechanical forces, independently of how veins form. This conclusion is supported by recent observations of vein development in young leaves and by the good quantitative agreement between our simulations and data from mature leaves.

Key words: Plant development, Mechanical stress

1 Introduction

Natural networks such as the vascular systems of plants and animals or river basins exhibit a strikingly regular, hierarchical structure, which has long been an object of scientific inquiry. In their study, two approaches can be distinguished, which address their organization in relation with their function or their development. This is true in particular of leaf venation networks (Roth-Nebelsick et al., 2001; Nelson and Dengler, 1997). Although they also serve for mechanical support (Niklas, 1999), the main function of leaf veins is fluid transport, and their structure can be interpreted in terms of optimal transport

properties (McCulloh et al., 2003; Durand, 2006) or tolerance to damage (Sack et al., 2008). As regards their development, new veins are formed progressively during leaf growth (Nelson and Dengler, 1997); while there is some evidence that the network is remodeled (through changes in relative vein size) as it develops (Kang and Dengler, 2004), its hierarchical organization largely reflects the history of its formation (Nelson and Dengler, 1997), which may thus be inferred by examining the thicknesses of its branches.

The development of veins involves the differentiation of ground cells into procambial (vein precursor) cells, which subsequently differentiate into the specialized tissues that make up the veins, and the reorganization of the network by coordinated growth. Here, "reorganization" refers to the progressive deformation of the network that results from the non-uniform growth of the leaf. The formation of veins is generally thought to be driven by the canalization of the hormone auxin (Sachs, 1981), although it was also proposed to involve mechanical stresses (Couder et al., 2002; Laguna et al., 2008). That the network undergoes reorganization during leaf development may be inferred from its geometrical properties in mature leaves (Bohn et al., 2002), and is apparent in the evolution of the network geometry in young leaves (Sawchuk et al., 2007), although it is seldom remarked upon. Moreover, if these geometrical properties can be understood as achieving an optimum in some sense, then reorganization is not a mere byproduct of growth, but a requirement for this optimum to be attained, and should be investigated alongside vein differentiation mechanisms to give a proper account of leaf venation morphogenesis. In the present study, leaving the question of vein differentiation aside, we propose a model in which veins are formed successively, and study how the network evolves through non-uniform growth driven by mechanical stresses. This model is most relevant to the leaves of dicots, one of two groups of flowering plants; monocots - the other group - exhibit different patterns of leaf growth and venation (Nelson and Dengler, 1997).

While the role of mechanical forces in plant growth is well established (Schopfer, 2006), and the importance of coordinated growth has been recognized in several areas of plant development (see e.g. Coen et al., 2004), the role of mechanical stresses as a patterning mechanism has received much less attention where plants are concerned (Green et al., 1996; Couder et al., 2002; Dumais, 2007; Laguna et al., 2008; Hamant et al., 2008) than in the study of animal development (see e.g. Farge, 2003; Hove et al., 2003; Nelson et al., 2005; Nguyen et al., 2006; Lecuit and Lenne, 2007; Hufnagel et al., 2007). This is true of experimental as well as modeling approaches, with most models of plant patterning involving biochemical mechanisms, in which auxin plays a prominent role. One notable exception is phyllotaxis (the arrangement of leaves or flowers on a stem): alongside biochemical models focusing on the transport of auxin (Jonsson et al., 2006; Smith et al., 2006; de Reuille et al., 2006), biomechanical models giving a central role to buckling under compressive forces have

also been proposed (Green et al., 1996). More recently, Newell et al. (2008) integrated the two approaches, showing that together they might ensure the stability of the obtained patterns, a matter left unresolved by otherwise successful models (Jonsson et al., 2006; Smith et al., 2006). Returning to leaf vein patterning, the role of growth is considered in some models (Runions et al., 2005; Fujita and Mochizuki, 2006), but most revolve around the auxin canalization hypothesis (e.g. Sachs, 1981; Mitchison, 1980; Dimitrov and Zucker, 2006; Feugier and Iwasa, 2006). To our knowledge, the only biomechanical approach was proposed by Laguna et al. (2008), who suggest that mechanical stresses induce differentiation; however, their model does not account for the reorganization of the vein network during growth, which we address here.

Veins in dicot leaves are typically laid out as follows: a midvein runs along the axis of the leaf, and secondary veins extend from the midvein to the margins; a reticulum formed of higher-order veins interconnects the secondary veins, dividing the surface of the leaf into areoles. The arrangement of the veins shows great variations among species (Hickey, 1973). This is particularly true of the largest veins, the layout of which is correlated with the shape of the leaf, and involves specific mechanisms (Scarpella et al., 2006). As regards the geometry of the higher-order veins, both visualization of cell identity markers in young leaves (Kang and Dengler, 2004; Scarpella et al., 2004, 2006; Wenzel et al., 2007; Sawchuk et al., 2007) and image analyses of vein skeletons in mature leaves (Bohn et al., 2002) suggest the reiteration of a self-organized process. Indeed, the local structure satisfies a universal property, which can be formulated as a simple vectorial equation which has been termed the "force model": if one associates with each vein a virtual force having the same direction as the vein and a magnitude proportional to its diameter, these forces are approximately balanced at each junction (Bohn et al., 2002). This result was found to hold across several species of dicotyledons.

To study the reorganization of venation networks, we developed a model incorporating well-established mechanisms of plant tissue growth. In this two-dimensional model, cell proliferation is driven by turgor pressure and two cell types are distinguished: ground cells and vein cells. The model is built upon the following rules, some of which are common in the modeling of plant growth (Prusinkiewicz and Lindenmayer, 1990; de Boer et al., 1992; Dupuy et al., 2008):

(1) cell walls are viscoelastic and elongate under turgor pressure;
(2) the mechanical properties of vein cells are different from those of ground cells; this assumption is essential as it induces the inhomogeneous mechanical stresses that drive the reorganization of the venation network;
(3) cells divide when they reach a threshold area;
(4) new veins appear when the areoles reach a threshold area.

This model is found to reproduce several qualitative and quantitative features of leaf venation geometry. We account for observations on young leaves (Scarpella et al., 2004, 2006; Sawchuk et al., 2007) as well as we recover the local geometrical properties of vein patterns in mature leaves (Bohn et al., 2002), quite independently of the details of the model. Overall, our results suggest that mechanical forces are important in shaping venation networks. Note however that, in contrast with the mechanism proposed by Couder et al. (2002) and implemented in the model of Laguna et al. (2008), in which mechanical stresses are involved in vein differentiation, they act here by driving the reorganization of the network. Indeed, while previous mechanical and biochemical models of vein patterning have focused on vein differentiation, we find that reorganization is essential in accounting for venation patterns. This conclusion is supported by the results of a simplified model, which shows how the effects of differentiation and reorganization may be separated in describing the formation of venation networks. The article is organized as follows: the model is detailed in Section 2; in Section 3, we give the results of the simulations and compare them to available experimental data; finally, in Section 4, we discuss the respective roles of differentiation and reorganization in leaf venation morphogenesis, and review the main hypotheses of our model, its limitations and its implications.

2 The model

We consider a single, two-dimensional layer of cells, represented as a partition of the plane into polygons. There are two cell types, ground and vein cells. As we are primarily interested in the local structure of the network, we consider a square, growing domain, with periodic boundary conditions.

2.1 Cell walls and growth

Plant cell growth is driven by the tensions induced in cell walls by turgor pressure (Schopfer, 2006). Cell walls respond to these tensions by a combination of elastic (reversible) and irreversible extension, the latter being identified with growth. To describe this process, Lockhart (1965) introduced a model in which elastic deformation is proportional to tension (Hooke's law) and growth rate is proportional to the tension in excess of a certain yield threshold. In our model, each wall i (corresponding in fact to the two walls that separate adjacent cells) is described as a viscoelastic rod with a time-dependent rest length l_i^0. Elastic deformation corresponds to the deviation between the actual length l_i of the wall and its rest length, and irreversible extension to the increase of the rest length with time. For simplicity, we assume that there is no growth threshold,

so that both are proportional to the tension T_i borne by the wall:

$$T_i = \mu h \left(\frac{l_i}{l_i^0} - 1 \right) = \frac{\nu_i h}{l_i^0} \frac{\mathrm{d}l_i^0}{\mathrm{d}t}. \tag{1}$$

Here h is the thickness of the wall, μ its elastic modulus, and ν_i its viscosity. We assume that all walls have the same elastic modulus μ and that cells actively maintain a constant wall thickness h through the addition of new material during elongation (Proseus et al., 1999; Cosgrove, 2005).

As noted by Lockhart (1965), elastic relaxation is much faster than growth, so that over the course of growth, elastic equilibrium is achieved at any given time (in other words, the evolution of the system is quasi-static). In this state of elastic equilibrium, the mechanical energy E of the system is minimized. In our simulations, a constant uniform turgor pressure P is assumed, so that E is given by

$$E = \sum_{i \in \text{walls}} \frac{\mu h l_i^0}{2} \left(\frac{l_i}{l_i^0} - 1 \right)^2 - \sum_{j \in \text{cells}} P S_j, \tag{2}$$

where S_j is the area of cell j. The first term corresponds to the elastic energy stored in the walls, which is proportional to the square of their elastic deformations. The second term is the pressure potential energy, which reflects the tendency of cells to swell under the effect of turgor (the potential energy becomes more negative when cell areas increase). More precisely, the variation of pressure potential energy when cell j changes size by ΔS_j is minus the work performed by the pressure inside cell j, which is equal to $P \Delta S_j$ (this is the two-dimensional equivalent of the work of pressure forces in three-dimensions, which is the pressure times the change of volume; the areas S_j can be seen as the volumes of cells in a tissue layer one unit length thick). The tendency of cells to swell under turgor is counteracted by the elasticity of their walls. At equilibrium, the two effects are exactly balanced.

To simulate the evolution of the system, we proceed as follows. At each time step, the state of the system (i.e., the positions of the junctions between walls) is determined by minimizing the mechanical energy E (with the rest lengths being fixed) using a conjugate-gradient algorithm, then the rest lengths l_i^0 are updated according to Eq. 1. Actually, with periodic boundary conditions, and for a large enough system, the assumption of a constant pressure is equivalent to that of a constant overall growth rate, which we have used for simplicity. Indeed, in that case, the pressure potential energy is independent of the configuration because the total area ($\sum_{j \in \text{cells}} S_j$) is fixed and can be ignored in the minimization.

2.2 The difference in mechanical properties of veins and ground tissue

Cells can actively control growth by the orientation of wall fibers and by expansins (Cosgrove, 2005). While ground cells have uniform, regular shapes, vein cells exhibit dramatic shape changes (Nelson and Dengler, 1997; Scarpella et al., 2006, 2004; Wenzel et al., 2007), which result from anisotropic growth and suggest anisotropic mechanical behavior. Consistent with this observation, we assume different mechanical properties for ground cell walls – uniform viscosity – and for vein walls – a higher viscosity that depends on the orientation of the wall relative to the vein to incorporate tissue anisotropy (walls between a vein cell and a ground cell are treated as vein walls). This hypothesis is all the more natural as mature vascular tissue is stiffer than the surrounding tissue (Niklas, 1999). Note that differences in elastic modulus (rather than viscosity) between ground and vein cells lead to similar results (see discussion).

The orientation dependence of vein wall behavior is described by introducing a measure of the local orientation of the vascular tissue, which is computed here as a function of the layout of the veins (and could be related to the local orientation of the elongated vein cells in actual leaves). Noting that such an orientation cannot be defined unambiguously within vein junctions, this measure must include information about the degree of anisotropy of the tissue as well as about its orientation. Mathematically, this can be done by representing the orientation by a symmetric, rank-two tensorial field. An intuitive interpretation of such a field is provided by the geometrical representation of its values in different locations by ellipses (see Fig. 2). The unambiguous orientation that can be defined away from junctions is indicated by elongated ellipses, the major axis of which is aligned with the direction of the vascular tissue, while the absence of a clear orientation in junctions is reflected by rounder ellipses. In more mathematical terms, the orientation tensor is defined such that its largest eigenvalue is always equal to one and the corresponding eigenvector is aligned with the direction of the tissue. The anisotropy is reflected by the ratio between the two eigenvalues of the tensor: the smallest eigenvalue is close to zero when the orientation is well defined, and becomes closer to one inside junctions.

While all ground cell walls share the same viscosity ν_g, the viscosity of each vein cell wall is a function of its direction and of the local orientation, such that:

- $\nu \simeq \lambda\nu_g$ ($\lambda > 2$) for an edge that is far from a junction and aligned with the local orientation.
- $\nu \simeq 2\nu_g$ for an edge that is far from a junction and perpendicular to the local orientation. On average, vein widths may thus be expected to increase at a rate that is half the overall growth rate of the system, which is roughly

consistent with the vein diameter distributions in leaves.
- ν varies continuously between these extremes for intermediate orientations.
- $\nu \simeq 2\lambda\nu_g$ inside vein junctions. This value is such that junctions grow at the same rate as the veins they connect.

The simulation results reported in what follows were obtained with $\lambda = 5$, which is the smallest value that yields effective reorganization. Larger values of λ give comparable results.

2.3 Cell division

Cells divide when they reach a threshold area ($S = 1$, defining our unit area), through the insertion of a new wall that is initially free of tension ($l_i = l_i^0$). The new wall runs through the centroid of the cell in the direction of the smallest second moment of area. This direction corresponds approximately to the smallest extension of the cell, similarly to proposed cell division criteria (Smith et al., 2006). The identity of cells (ground/vein) is inherited during divisions.

2.4 Areole division

The simulation begins with a small number of ground cells. Veins are added progressively over time, by switching files of ground cells to the vein state. The first two veins are placed arbitrarily, forming a first areole (this is possible due to the periodic boundary conditions). Subsequently, new veins are added when an areole reaches a threshold area (S_a), dividing it into smaller areoles. As a simplification, there are no freely-ending veins. The value $S_a = 100$ was chosen based on an estimate of the number of cells in areoles in developing *Arabidopsis* leaves (see e.g. Scarpella et al., 2004). The time when the first veins are created is such that the area of the first areole is of the order of $S_a/2$, as if it were formed by the division of a larger areole.

The locations of new veins are determined according to geometrical rules that are qualitatively consistent with the auxin canalization hypothesis (Sachs, 1981), yet compatible with other vein patterning models (e.g. the mechanical model of Couder et al., 2002). When an areole is divided, several new veins connecting the center of the areole to its boundary are added successively. The locations of the new veins are chosen such that they are more or less evenly distributed while keeping their length to a minimum. More specifically, each new vein connects the center C of the areole to the point along its boundary that maximizes a function f, where f is inversely proportional to the distance to the center and penalizes points that are close to previously added veins. If

M_i are the ends of previous veins (see Fig. 1C), the value of f at a point M is given by

$$f(M) = \frac{\Pi_i g\left(\left|\overrightarrow{M_i M}\right|\right)}{\left|\overrightarrow{MC}\right|}, \tag{3}$$

where g is a function satisfying $g(0) = 0$ and $g(x) \to 1$ when $x \to +\infty$. This procedure can be seen as a crude implementation of the auxin canalization hypothesis as presented by Dimitrov and Zucker (2006): f may be understood as an estimate of the auxin flux, where g models the reduction in flux due to auxin depletion from other veins; new veins connect a maximum of auxin flux to the center of the areole. New veins are added until the maximum of f along the boundary of the areole no longer exceeds a certain threshold. With the threshold value used here, areoles are divided in two or three according to their shape (Fig. 1, D and E): elongated areoles are typically divided in two along their shortest extension, while areoles that have a rounder shape are divided in three (Fig. 1, D and E). New veins are continuously added until the system reaches a certain size ($L \approx 55.5$), then growth alone continues until it reaches its final size ($L \approx 113$), mimicking late stages of leaf development (Rolland-Lagan et al., 2009).

3 Results

3.1 Evolution of the network

Figure 3 shows a sequence illustrating several stages of a typical run. As the system grows, a continuous reorganization of the vein network is observed. Firstly, the veins, which initially have the form of an irregular file of cells, tend to become straighter between vein junctions, as do their boundaries. Secondly, the network deforms progressively, giving rise to zigzagging vein paths similar to those observed in actual young leaves (see e.g. Fig. 3J in Scarpella et al., 2004).

These observations can be explained in light of the mechanical properties of vein cells. To maintain tissue integrity, each vein must stretch longitudinally at the same rate as the surrounding tissue, and the higher viscosity results in increased longitudinal tensions. On the one hand, these tensions tend to straighten out veins and their boundaries. On the other hand, the average tension along a vein is proportional to the number of walls oriented in the longitudinal direction (the strain rates of these walls, and thus their tensions, are approximatively uniform), and thus to the width of the vein (the walls are evenly separated). The reorganization leads to a state such that the tensions are balanced at a given junction, imposing a relation between the widths of the

veins and the angles between them. This gives a rationale for the balance of virtual forces introduced in Bohn et al. (2002) to describe the geometry of junctions. The outcome of the evolution is a netted hierarchical structure (Fig. 3C) that is visually similar to the local structure of a mature leaf (Fig. 3D).

3.2 Geometry of the network

To allow a quantitative comparison, the simulation was run repeatedly with randomized initial conditions, and the statistical properties of the patterns obtained were analyzed. The hierarchical structure of the networks is reflected by the distribution of veins widths (Fig. 4B) – a wide distribution – and the relation between the widths at junctions (Fig. 4C) – thin veins connect to thick veins.

Now, the overall structure of the network is mostly a reflection of the rules used to add new veins. More importantly, we find that the local structure of the network that results from its reorganization is in good agreement with measurements on mature leaves (Bohn et al., 2002). The angles at junctions are broadly distributed (Fig. 4D), varying continuously between values similar to those observed in crack patterns ($90^\circ + 90^\circ + 180^\circ$), found when a thin vein connects to thick veins, and to those observed in two-dimensional soap froths ($120^\circ + 120^\circ + 120^\circ$), for veins having comparable sizes (Fig. 4E). This is consistent with the force model: a very thin vein develops a small tension, so that the balance of forces between the intermediate and larger vein tends to align them, yielding the crack-like limit; three veins of the same thickness have the same tension, so that force balance imposes angles of 120° between them, which is the froth-like limit.

All of the above measures of network structure show good quantitative agreement between our simulations and actual leaves (Bohn et al., 2002), confirming that our model yields patterns that are geometrically similar to actual leaf venation networks, as regards in particular the geometry of vein junctions.

4 Discussion

We have described the reorganization of leaf venation networks on the basis of the biophysical properties of plant cells, while vein differentiation is implemented summarily in the form of geometrical rules. To demonstrate that the two can indeed be separated in accounting for the local structure of the networks, we performed additional simulations.

On the one hand, we switched off the difference in mechanical properties between vein and ground cells. The resulting patterns are irregular (Fig. 5A); the veins remain wavy with irregular boundaries. This illustrates the importance of non-uniform mechanical properties within the leaf. On the other hand, we developed a simplified model in which vein segments are represented as straight lines of constant width, dividing the leaf into polygonal areoles (see Fig. 5, B and C). Veins are added according to the geometrical rules for areole division used above and their widths increase at a constant rate. In a first version of this simplified model, growth is uniform with no reorganization, and the development of the network reduces to successive areole division (Fig. 5B). The angle distribution is very different in this case: most junctions contain a 180° angle (Fig. 5E). Note that this does not preclude correlations between vein sizes and angles. Such correlations were in fact observed by Laguna et al. (2008) in their mechanical model of vein differentiation, and led them to claim that their model could account for the geometry of vein junctions. However, only a small fraction of vein junctions can be expected to contribute to junction geometries other than a crack-like one - and to these correlations - in a model that does not include reorganization, in contrast with the broad angle distributions observed in our model and in plant leaves.

In a second version of the simplified model, each vein segment behaves as a viscoelastic rod. We use the same equations as for the cell proliferation model (Eqs. 1-2). This can be viewed as the limit of the cell proliferation model where the viscosity of ground cells is negligible. Fig. 5C shows a resulting pattern, which is very similar to Fig. 3C. The reorganization manifests itself by a broad distribution of the angles between veins (Fig. 5F), as in the full model (Fig. 4D) and as is observed in mature leaves (Bohn et al., 2002). We also investigated the effect of modifying the rules for areole division (Fig. 5D): dividing all areoles in two (rather than in two or three depending on their shape), while it decreases the number of froth-like junctions, does not substantially change the correlations between vein angles and widths (Fig. 5G). These results show that the local structure of the network is determined by its reorganization, and essentially independent of the mechanism of vein differentiation, confirming that it is governed by the mechanics of growth, provided that the rheological properties of vein and ground cells differ. Note that differences in rheology do not affect the shape of future vein cells instantaneously, but over the course of growth, which explains why shape changes are not observed at the earliest stages of vein patterning.

Let us finally discuss the generality of our cell proliferation model applied to leaf venation. Consideration of the actual cylindrical shape of veins would suggest that the tensions should be proportional to the cross-section of the veins; this apparent contradiction with the virtual force model (Bohn et al. (2002) found the virtual forces to be proportional to vein diameter) could be resolved if the mechanical behavior of veins is dominated by the bundle sheath

(a layer of cells that surrounds the vein). The rest of our results is mostly insensitive to the details of the model: rheology of the walls, cell shapes and division rules. For instance, if the elastic modulus of vein cells is higher, but their viscosity is the same as those of ground cells, comparable elastic strains are associated with comparable growth rates of the two cell types, but would correspond to higher tensions in vein cells, as with the differences in viscosity assumed here. In both cases, the net result on the tissue level is that different tensions are needed to achieve a given growth rate, which is the key to the proposed reorganization mechanism. The same effect could also result from the elongated shapes of vein cells, which increase the density of cell walls in veins. However, the consequences of the shape of vein cells on their mechanical behavior could be described properly only within a three-dimensional model (which is why we did not attempt to reproduce them; the growth of vein cells in our model is in fact anisotropic but cell elongation is limited by transverse cell divisions, while it is amplified in actual leaves by longitudinal divisions). These effects are most probably combined in actual leaves.

Robustness of the model is warranted by the small number of relevant parameters: viscosity ratios and areole to cell threshold area ratio. In addition, these parameters are largely constrained. The ratio of areole threshold area to cell threshold area is readily measurable in actual leaves. As we have noted, the viscosity of vein cells in the transverse direction is related to the distribution of vein widths, and we chose a value consistent with the observed distribution. That this viscosity should be higher than that of ground cells can be concluded from the fact that leaf veins become more elongated with time, indicating that the growth of vein diameters is slower than the overall growth of the leaf. On the other hand, if it was much larger than one, vein diameters would barely increase with time, and the hierarchical structure of the network would be lost. As regards the longitudinal viscosity of vascular cells, if it is decreased below the value used here ($\lambda = 5$), veins become gradually more irregular and reorganization less effective. Larger values yield comparable results. Overall, our model is in agreement with statistical data on mature leaves, and predicts a reorganization that is already visible at the early stages of development (Kang and Dengler, 2004; Scarpella et al., 2004, 2006), in particular in the time-lapse images by Sawchuk et al. (2007), e.g. Fig. 3(i), in which an initially straight vein that develops a kink after a new vein has connected to it is clearly visible. While it seems hardly feasible to probe the mechanical behavior of individual differentiating vascular cells, we predict that the application of mechanical forces to growing leaves should influence the venation network, which suggests a indirect route to investigate this behavior and obtain further experimental evidence of its importance in leaf development.

While it was essential to our conclusions to show how differentiation and growth could be separated, both aspects would have to be reunited to give a more comprehensive account of leaf venation morphogenesis. To do so, the ge-

ometrical rules used in our model to describe the formation of veins would have to be replaced by a suitable model of vein differentiation, whether mechanical or biochemical. In this perspective, it must be noted that existing biochemical models of vein differentiation are usually formulated on the cellular scale, and could readily be integrated with our approach. Also, we considered periodic boundary conditions to investigate the local structure of leaf venation networks, and a reticular network structure, but our model would be equally applicable to the different network structures that could be generated with other differentiation rules, e.g. branched networks, or to an entire leaf. Finally, the mechanisms of vein differentiation may provide a clue to the origin of the anisotropy of vein cell behavior. This was implemented geometrically in our model, by constructing a local orientation from the shape of the veins, leaving open the question of how actual cells might "perceive" the orientation of veins. One could imagine that this response involves the polar transport of auxin. Indeed, the localization of PIN (auxin efflux carrier) proteins is one of the earliest signs of a preferential orientation in differentiating vascular tissue (see e.g. Scarpella et al., 2006). Overall, this points to the integration of cell-level molecular processes with tissue-level coordinated growth as a promising direction for future investigation of plant morphogenesis.

Acknowledgments

We thank Steffen Bohn for the data on mature leaves and fruitful discussions, and Jacques Dumais, Hervé Henry and Olivia Puttman for fruitful discussions. This work was supported by European Union NEST Adventure Mechplant.

Appendix. Supplementary materials

Movie of the evolution of the cell proliferation model corresponding to Fig. 3.

References

Bohn, S., Andreotti, B., Douady, S., Munzinger, J., Couder, Y., 2002. Constitutive property of the local organization of leaf venation networks. Phys. Rev. E 65, 061914.

Coen, E., Rolland-Lagan, A. G., Matthews, M., Bangham, J. A., Prusinkiewicz, P., 2004. The genetics of geometry. PNAS 101, 4728–4735.

Cosgrove, D. J., 2005. Growth of the plant cell wall. Nat. Rev. Mol. Cell Biol. 6, 850–861.

Couder, Y., Pauchard, L., Allain, C., Adda-Bedia, M., Douady, S., 2002. The leaf venation as formed in a tensorial field. Eur. Phys. J. B 28, 135–138.

de Boer, M. J. M., Fracchia, F. D., Prusinkiewicz, P., 1992. Lindenmayer Systems: Impacts on Theoretical Computer Science, Computer Graphics, and Developmental Biology. Springer-Verlag, Ch. A model for cellular development in morphogenetic fields.

de Reuille, P. B., Bohn-Courseau, I., Ljung, K., Morin, H., Carraro, N., Godin, C., Traas, J., 2006. Computer simulations reveal properties of the cell-cell signaling network at the shoot apex in Arabidopsis. PNAS 103, 1627–1632.

Dimitrov, P., Zucker, S. W., 2006. A constant production hypothesis guides leaf venation patterning. PNAS 103, 9363–9368.

Dumais, J., 2007. Can mechanics control pattern formation in plants? Curr. Opin. Plant Biol. 10, 58–62.

Dupuy, L., Mackenzie, J., Rudge, T., Haseloff, J., 2008. A system for modelling cell-cell interactions during plant morphogenesis. Ann. Bot. 101, 1255–1265.

Durand, M., 2006. Architecture of optimal transport networks. Phys. Rev. E 73, 016116.

Farge, E., 2003. Mechanical induction of Twist in the Drosophila foregut/stomodeal primordium. Curr. Biol. 13, 1365–1377.

Feugier, F. G., Iwasa, Y., 2006. How canalization can make loops: A new model of reticulated leaf vascular pattern formation. J. Theor. Biol. 243, 235–244.

Fujita, H., Mochizuki, A., 2006. The origin of the diversity of leaf venation pattern. Dev. Dynam. 235, 2710–2721.

Green, P. B., Steele, C. S., Rennich, S. C., 1996. Phyllotactic patterns: A biophysical mechanism for their origin. Ann. Bot. 77, 515–527.

Hamant, O., Heisler, M., Jonsson, H., Krupinski, P., Uyttewaal, M., Bokov, P., Corson, F., Sahlin, P., Boudaoud, A., Meyerowitz, E., Couder, Y., Traas, J., 2008. Developmental patterning by mechanical signals in Arabidopsis. Science 322, 1650–1655.

Hickey, L. J., 1973. Classification of the architecture of dicotyledonous leaves. Am. J. Bot. 60, 17–33.

Hove, J. R., Koster, R. W., Forouhar, A. S., Acevedo-Bolton, G., Fraser, S. E., Gharib, M., 2003. Intracardiac fluid forces are an essential epigenetic factor for embryonic cardiogenesis. Nature 421, 172–177.

Hufnagel, L., Teleman, A. A., Rouault, H., Cohen, S. M., Shraiman, B. I., 2007. On the mechanism of wing size determination in fly development. PNAS 104, 3835–3840.

Jonsson, H., Heisler, M. G., Shapiro, B. E., Meyerowitz, E. M., Mjolsness, E., 2006. An auxin-driven polarized transport model for phyllotaxis. PNAS 103, 1633–1638.

Kang, J., Dengler, N., 2004. Vein pattern development in adult leaves of Arabidopsis thaliana. Int. J. Plant Sci. 165, 231–242.

Laguna, M. F., Bohn, S., Jagla, E. A., 2008. The role of elastic stresses on leaf venation morphogenesis. PLoS Comput. Biol. 4, e1000055.

Lecuit, T., Lenne, P. F., 2007. Cell surface mechanics and the control of cell

shape, tissue patterns and morphogenesis. Nat. Rev. Mol. Cell Biol. 8, 633–644.

Lockhart, J. A., 1965. An analysis of irreversible plant cell elongation. J. Theor. Biol. 8, 264–275.

McCulloh, K. A., Sperry, J. S., Adler, F. R., 2003. Water transport in plants obeys Murray's law. Nature 421, 939–942.

Mitchison, G. J., 1980. A model for vein formation in higher plants. Proc. R. Soc. Lond. B 207, 79–109.

Nelson, C. M., Jean, R. P., Tan, J. L., Liu, W. F., Sniadecki, N. J., Spector, A. A., Chen, C. S., 2005. Emergent patterns of growth controlled by multicellular form and mechanics. PNAS 102, 11594–11599.

Nelson, T., Dengler, N., 1997. Leaf vascular pattern formation. Plant Cell 9, 1121–1135.

Newell, A. C., Shipman, P. D., Sun, Z. Y., 2008. Phyllotaxis: Cooperation and competition between mechanical and biochemical processes. J. Theor. Biol. 251, 421–439.

Nguyen, T. H., Eichmann, A., Le Noble, F., Fleury, V., 2006. Dynamics of vascular branching morphogenesis: The effect of blood and tissue flow. Phys. Rev. E 73, 061907.

Niklas, K. J., 1999. A mechanical perspective on foliage leaf form and function. New Phytol. 143, 19–31.

Proseus, T. E., Ortega, J. K. E., Boyer, J. S., 1999. Separating growth from elastic deformation during cell enlargement. Plant Physiol. 119, 775–784.

Prusinkiewicz, P., Lindenmayer, A., 1990. The Algorithmic Beauty of Plants. Springer-Verlag, Ch. 7.

Rolland-Lagan, A.-G., Amin, M., Pakulska, M., 2009. Quantifying leaf venation patterns: two-dimensional maps. Plant J. 57, 195–205.

Roth-Nebelsick, A., Uhl, D., Mosbrugger, V., Kerp, H., 2001. Evolution and function of leaf venation architecture: A review. Ann. Bot. 87, 553–566.

Runions, A., Fuhrer, M., Lane, B., Federl, P., Rolland-Lagan, A. G., Prusinkiewicz, P., 2005. Modeling and visualization of leaf venation patterns. ACM T. Graphic. 24, 702–711.

Sachs, T., 1981. The control of the patterned differentiation of vascular tissues. Adv. Bot. Res. 9, 151–262.

Sack, L., Dietrich, E. M., Streeter, C. M., Sanchez-Gomez, D., Holbrook, N. M., 2008. Leaf palmate venation and vascular redundancy confer tolerance of hydraulic disruption. PNAS 105, 1567–1572.

Sawchuk, M. G., Head, P., Donner, T. J., Scarpella, E., 2007. Time-lapse imaging of Arabidopsis leaf development shows dynamic patterns of procambium formation. New Phytol. 176, 560–571.

Scarpella, E., Francis, P., Berleth, T., 2004. Stage-specific markers define early steps of procambium development in Arabidopsis leaves and correlate termination of vein formation with mesophyll differentiation. Development 131, 3445–3455.

Scarpella, E., Marcos, D., Friml, J., Berleth, T., 2006. Control of leaf vascular

patterning by polar auxin transport. Gene. Dev. 20, 1015–1027.
Schopfer, P., 2006. Biomechanics of plant growth. Am. J. Bot. 93, 1415–1425.
Smith, R. S., Guyomarc'h, S., Mandel, T., Reinhardt, D., Kuhlemeier, C., Prusinkiewicz, P., 2006. A plausible model of phyllotaxis. PNAS 103, 1301–1306.
Wenzel, C. L., Schuetz, M., Yu, Q., Mattsson, J., 2007. Dynamics of MONOPTEROS and PIN-FORMED1 expression during leaf vein pattern formation in Arabidopsis thaliana. Plant J. 49, 387–398.

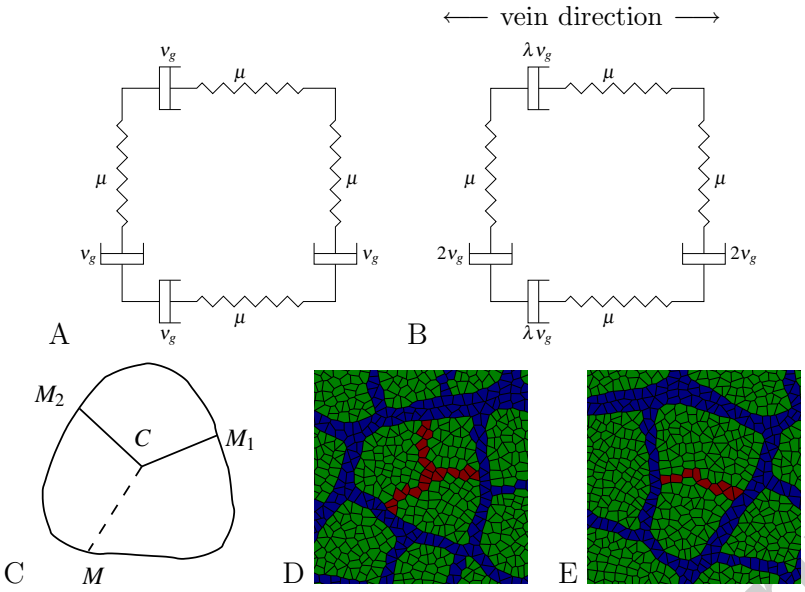

Fig. 1. Principle of the cell proliferation model. (**A**, **B**) Cells have viscoelastic walls (represented as a spring in series with a dashpot) and grow under turgor pressure. For simplicity, square cells are represented. All walls have the same elastic modulus μ. Ground cell walls (**A**) have viscosity ν_g. Vein cell walls (**B**) perpendicular (resp. parallel) to the vein have viscosity $2\nu_g$ (resp. $\lambda\nu_g$ with $\lambda > 2$). (**C**,**D**,**E**) Areole division rules. New veins are added when an areole reaches a threshold area (see text for details). (**C**) Diagram defining the points used in Eq. 3 (**D**,**E**) Ground cells and vein cells are shown as green and blue polygons, respectively, while the black lines indicate the locations of cell walls. Newly added veins are highlighted in red. (**D**) A roughly round areole is divided in three. (**E**) An elongated areole is divided in two along its shortest extension (this is similar to the cell division rule).

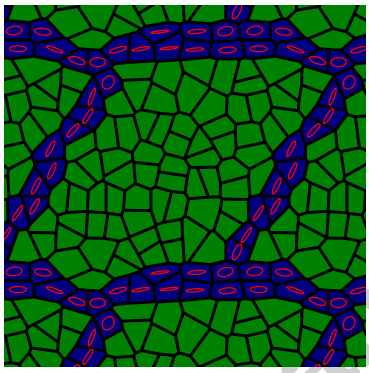

Fig. 2. Local orientation of the vascular tissue, which governs the anisotropic mechanical behavior of vascular cells (see text). Note that this orientation is defined according to the layout of the veins, and does not necessarily coincide with the orientation of individual cells (which determines their division planes). It is mathematically defined as a tensorial field, which can be represented by ellipses. The unambiguous orientation that can be defined away from junctions is reflected by elongated ellipses, while the absence of a clear orientation within junctions is reflected by rounder ellipses.

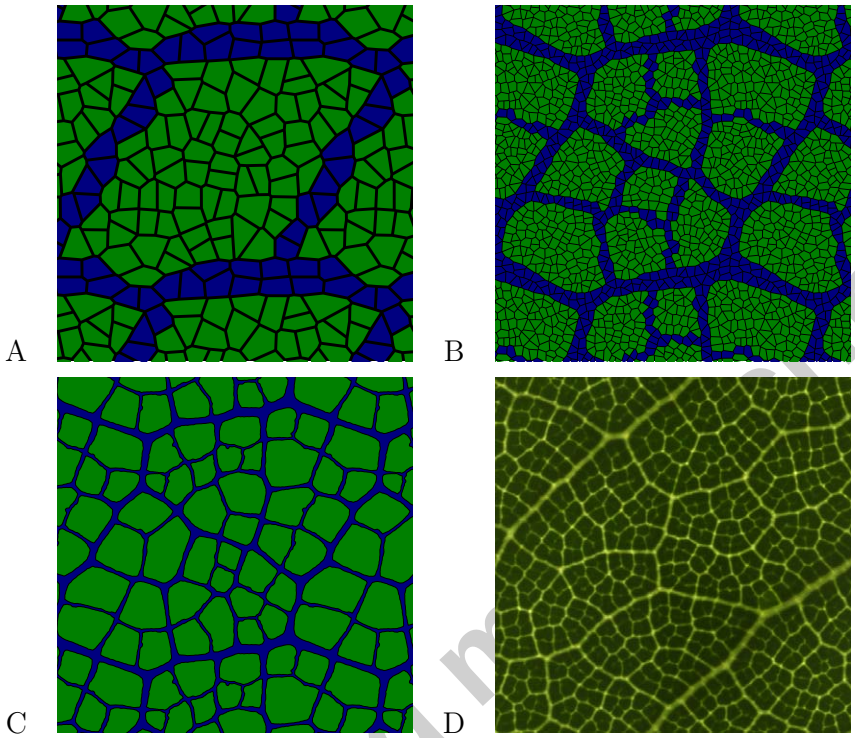

Fig. 3. (**A**,**B**,**C**) Development of venation patterns in the cell proliferation model (colors same as Fig. 1). See Supporting online material for a movie. For each image, we indicate the size L of the periodic pattern and show an area $1.5L \times 1.5L$ (the unit length is given by the threshold area $S = 1$ for cell division). (**A**) State when the first veins have been added ($L \simeq 8$). (**B**) Later stage of growth ($L \simeq 25$). Newly added veins appear as irregular rows of cells. Vein segments formed earlier are straighter and have smoother boundaries. (**C**) End of the simulation ($L \simeq 113$; individual cells are not shown). Notice how the angles between veins evolve with time. (**D**) Detail of the venation network of a mature *Pittosporum* leaf (14mm x 14mm).

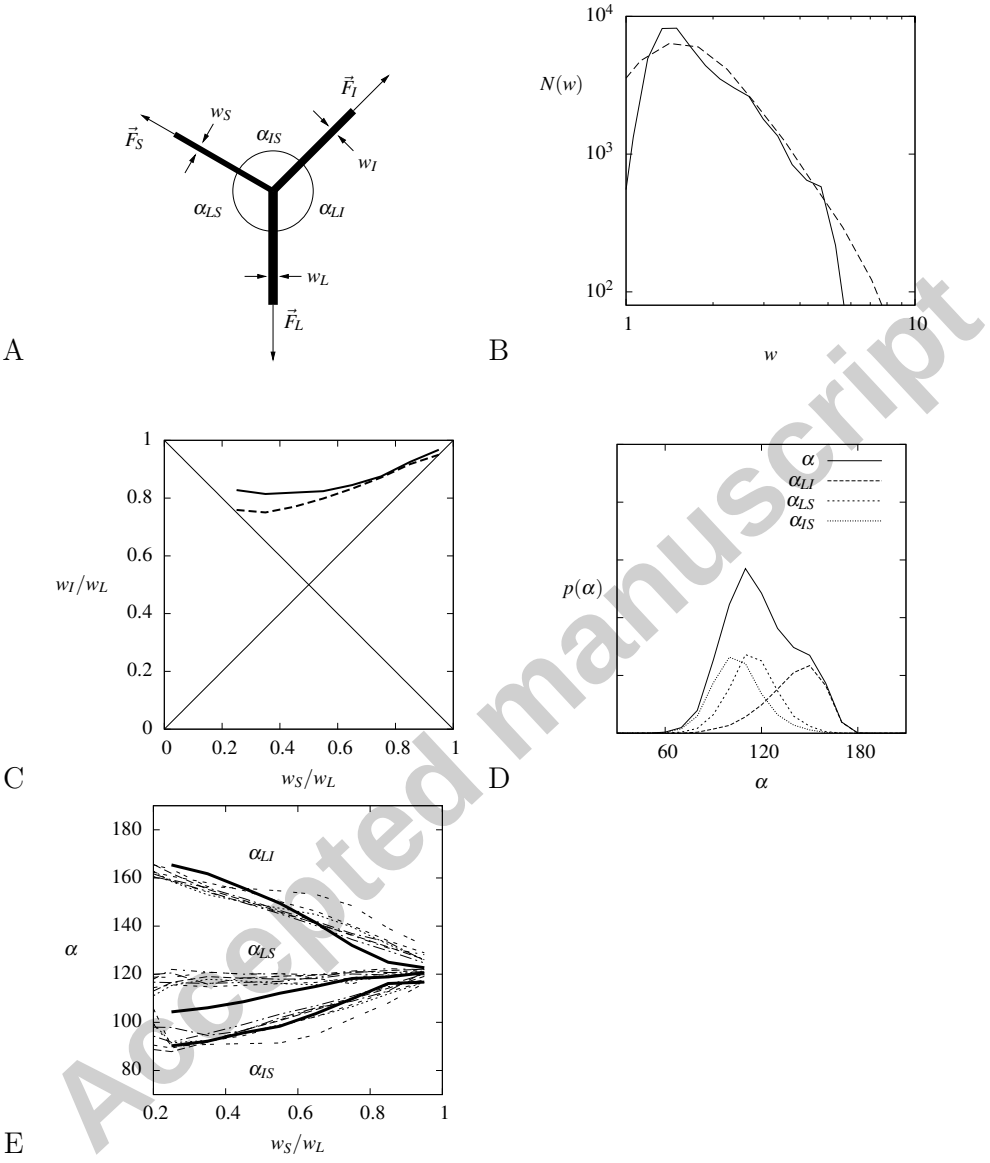

Fig. 4.

Fig. 4. Geometrical properties of the vein network. (**A**) At each junction, the veins are labeled according to their width as large (L), intermediate (I), and small (S). The parameters used to describe the junction are the widths $w_{L,S,I}$, the angles $\alpha_{LI,LS,IS}$, and the virtual forces $\vec{F}_{L,S,I}$ having magnitudes proportional to the widths of the veins. (**B**) Distribution of veins widths. Simulation (bold line) and data from Bohn et al. (2002) for leaves of *Gloeospermum* (dashed line; in that case, the unit length is 20μm, which is of the order of one cell size). Due to numerical limitations, the distribution of vein widths in the simulations is not as broad as that in actual leaves, which extends beyond the limits of the figure. (**C**) Correlation between the widths: average of w_I/w_L versus w_S/w_L. Simulation (bold line) and data from Bohn et al. (2002) for leaves of *Gloeospermum* (dashed line). The two straight lines $w_I = w_S$ and $w_I + w_S = w_L$ are limits imposed by the definition $w_I \geq w_S$ and by the force balance $\vec{F}_I + \vec{F}_S + \vec{F}_L = \vec{0}$. (**D**) Distributions of the angles between veins in the simulations. (**E**) Correlations between the angles and widths: averages of α_{LI}, α_{LS}, α_{IS} versus w_S/w_L. Simulation (bold lines) and data from Bohn et al. (2002) for leaves of several species (other lines). The variation of α_{LI} is a signature of the force model. The geometry of junctions was analyzed as in Bohn et al. (2002); junctions between more than three veins (which are rare) or too close to another junction (separated by a distance smaller than the width of the connecting segment) were discarded.

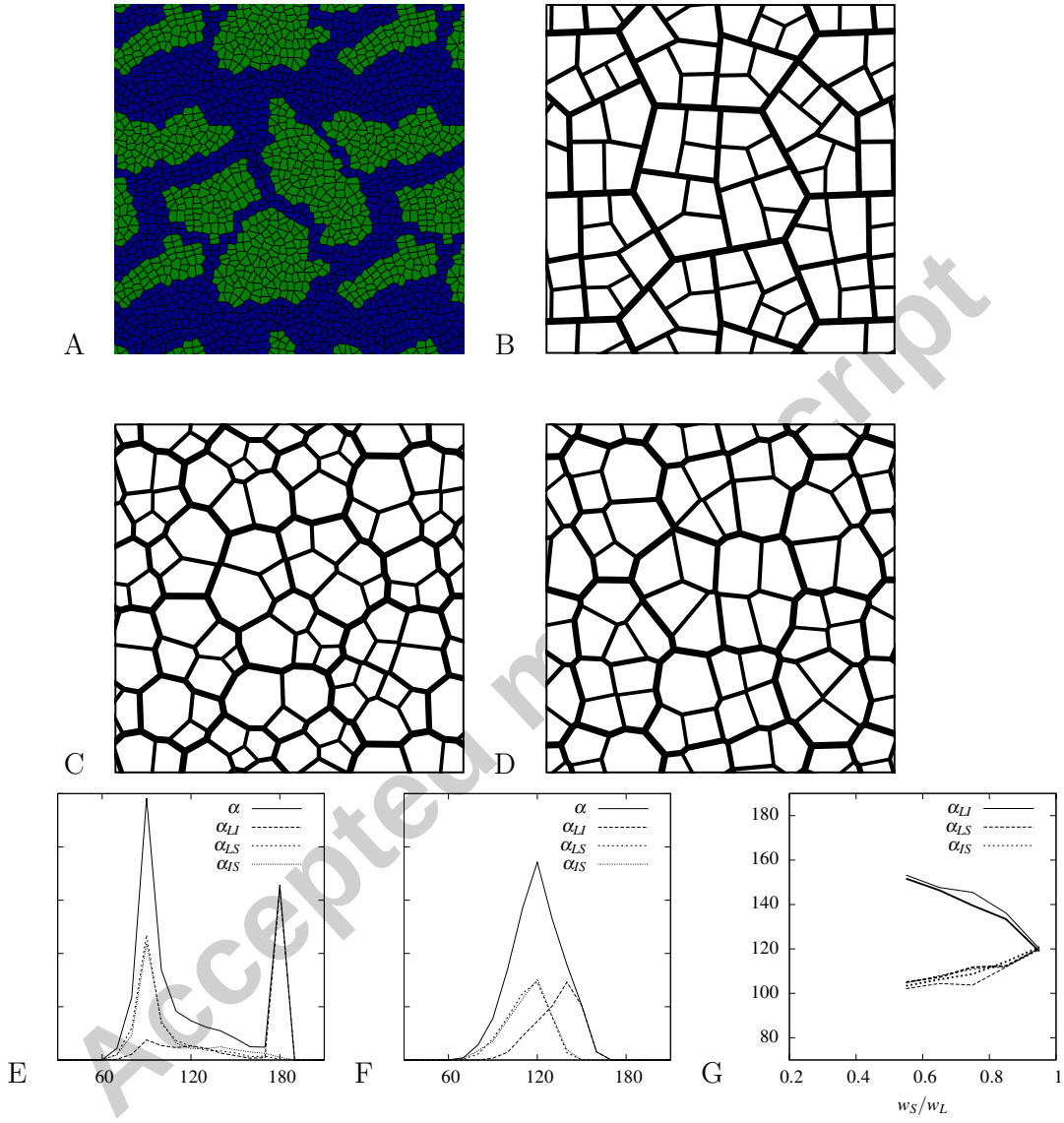

Fig. 5.

Fig. 5. Importance of coordinated growth driven by mechanical stresses. (**A**) Cell proliferation model where ground and vein cells have the same mechanical properties, yielding a disorganized pattern. (**B**) Simplified model with uniform growth, yielding only crack-like junctions. (**C**) Simplified model with reorganization, with results very similar to the full model, as in Fig. 3C. (**D**) Simplified model with reorganization and all areoles divided in two. (**E**) Angle distributions in the simplified model with uniform growth shown in A are peaked near 90° and 180°, with the less frequent intermediate values resulting from vein junctions formed by the division of an areole in three. (**F**) Angles in the simplified model with reorganization shown in C are broadly distributed, as in the full model (Fig. 4D) and in leaves (Bohn et al., 2002). (**G**) Correlations between veins widths and angles in the simplified model with reorganization shown in C (bold lines) and in the simplified model with altered division rules shown in D (thin lines); same notations as in Fig. 4E.